arXiv:1303.7192v3 [nucl-th] 9 Apr 2013

Axial Current Generation from Electric Field: Chiral Electric Separation Effect

Xu-Guang Huang[1, *] and Jinfeng Liao[1, 2, †]

[1] *Physics Department and Center for Exploration of Energy and Matter,*
Indiana University, 2401 N Milo B. Sampson Lane, Bloomington, IN 47408, USA.
[2]*RIKEN BNL Research Center, Bldg. 510A, Brookhaven National Laboratory, Upton, NY 11973, USA.*

(Dated: April 11, 2013)

We study a relativistic plasma containing charged chiral fermions in an external electric field. We show that with the presence of both vector and axial charge densities, the electric field can induce an axial current along its direction and thus cause chirality separation. We call it the Chiral Electric Separation Effect (CESE). On very general basis, we argue that the strength of CESE is proportional to $\mu_V\mu_A$ with μ_V and μ_A the chemical potentials for vector charge and axial charge. We then explicitly calculate this CESE conductivity coefficient in thermal QED at leading-log order. The CESE can manifest a new gapless wave mode propagating along the electric field. Potential observable of CESE in heavy-ion collisions is also discussed.

PACS numbers: 11.40.Ha,12.38.Mh,25.75.Ag

Introduction.—It was discovered and understood a long time ago that an external electric field, when applied to any conducting matter, induces a vector current, as described by the Ohm's law

$$\boldsymbol{j}_V = \sigma \boldsymbol{E}, \tag{1}$$

where σ is the electric conductivity of the matter and we use the convention that the electric current is $e\boldsymbol{j}_V$. In quantum field theories such as the Quantum Electrodynamics (QED) and the Quantum Chromodynamics (QCD), one has not only the vector current j_V^μ but also the axial current j_A^μ when there are charged chiral fermions. A very interesting question is then, in addition to the above conducting vector current under applied electric field, what are the other possible current generations in response to externally applied Maxwell electric and/or magnetic fields.

Recently, the QCD axial anomaly has been found to induce the following two phenomena in the high-temperature deconfined phase of QCD, the quark-gluon plasma (QGP), with the presence of an external magnetic field: the Chiral Magnetic Effect (CME) and the Chiral Separation Effect (CSE). The CME is the generation of vector current and thus the electric charge separation along the axis of the applied magnetic field in the presence of nonzero axial charge density arising from fluctuating topological charge [1–5]. With an imbalance between the densities of left- and right-handed quarks, parameterized by an axial chemical potential μ_A, an external magnetic field induces the vector current $j_V^i = \langle\bar\psi\gamma^i\psi\rangle$:

$$\boldsymbol{j}_V = \sigma_5 \mu_A \boldsymbol{B}; \tag{2}$$

with chiral conductivity $\sigma_5 \equiv \frac{N_c e}{2\pi^2}$. A "complementary" effect also arising from the axial anomaly is the CSE which predicts the generation of an axial current, $j_A^i = \langle\bar\psi\gamma^i\gamma_5\psi\rangle$, and thus separation of axial charges along the external $\boldsymbol{B}$ field at nonzero vector charge density (parameterized by its chemical potential μ_V) [6, 7]:

$$\boldsymbol{j}_A = \sigma_5 \mu_V \boldsymbol{B}. \tag{3}$$

There are robust evidences for both CME and CSE from kinetic theory, hydrodynamics, holographic QCD models in strong coupling regime as well as in lattice QCD computations [8–19]. Experimentally the hot QGP is created in high energy heavy ion collisions at the Relativistic Heavy Ion Collider (RHIC) and the Large Hadron Collider (LHC). In such collisions,domains of QGP with nonzero chirality ($\mu_A \neq 0$) can arise from topological transitions in QCD and there are also extremely strong transient $\boldsymbol{E}$ and $\boldsymbol{B}$ fields [20–24], so the CME and CSE effects can occur. There have been measurements of charge asymmetry fluctuations motivated by CME predictions from the STAR [25] and PHENIX [26] Collaborations at RHIC as well as from the ALICE [27] at LHC. The precise meaning of these data is under investigations, see e.g. [28]. It has also been proposed that the combination of the CME and CSE leads to a collective excitation in QGP called Chiral Magnetic Wave (CMW) [29]. The CMW induces an electric quadruple of QGP that can be measured via elliptic flow splitting between negative/positive pions [30], with very supportive evidences from recent STAR measurements [31].

There is, however, one more possibility that has not been previously discussed, namely the generation of an axial current in the electric field. We find this to occur when the matter has both nonzero μ_V and nonzero μ_A:

$$\boldsymbol{j}_A = \chi_e \mu_V \mu_A \boldsymbol{E}, \tag{4}$$

which can be called a *Chiral Electric Separation Effect* (CESE). In this Letter, we will derive this relation, and explicitly compute the CESE conductivity χ_e in thermal QED. With this new relation found, one can nicely combine all four effects into the following form:

$$\begin{pmatrix} \boldsymbol{j}_V \\ \boldsymbol{j}_A \end{pmatrix} = \begin{pmatrix} \sigma & \sigma_5\mu_A \\ \chi_e\mu_V\mu_A & \sigma_5\mu_V \end{pmatrix} \begin{pmatrix} \boldsymbol{E} \\ \boldsymbol{B} \end{pmatrix}. \tag{5}$$

Chiral Electric Separation Effect.— To intuitively understand how the CESE (4) arises, let us consider a conducting system with chiral fermions. When an electric field is applied, the positively/negatively charged fermions will move parallel/anti-parallel to the $\boldsymbol{E}$ direction and both contribute to the total vector current as in Eq.(1). If $\mu_V > 0$ then there will be more positive fermions (who are moving along $\boldsymbol{E}$) and if further $\mu_A > 0$ then there will be more right-handed fermions than the left-handed ones, there will thus be a net flux of right-handed (positive) fermions moving parallel to $\boldsymbol{E}$. This picture is most transparent in the extreme situation when the system contains only right-handed fermions (i.e. in the limit of $\mu_V = \mu_A > 0$), then it is obvious that there will be both a vector current and an axial current generated in parallel to $\boldsymbol{E}$. The same conclusion can be made when both μ_V and μ_A are negative. In cases with $\mu_V > 0 > \mu_A$ or $\mu_V < 0 < \mu_A$ one can follow the same line of argument to see an axial current generated in anti-parallel to the $\boldsymbol{E}$ direction.

Different from the CME and CSE, the generation of axial current via CESE is not related to axial anomaly, but rather arising from the same conducting transport responsible for usual conduction in Eq.(1). To demonstrate that, let us consider the conduction of left-handed fermions, $\boldsymbol{j}_L = \sigma(T;\mu_L,\mu_R)\boldsymbol{E}$ where $\mu_L = \mu_V - \mu_A$ and $\mu_R = \mu_V + \mu_A$ are the left-handed and right-handed chemical potentials, respectively. Due to symmetry reason, the conducting current of right-handed fermions must be $\boldsymbol{j}_R = \sigma(T;\mu_R,\mu_L)\boldsymbol{E}$. We focus on the situation when all chemical potentials are small comparing to the temperature T, so that $\sigma(T;\mu_L,\mu_R) \approx \sigma_0(T)+\sigma_0'(T)\mu_L^2+\sigma_0''(T)(\mu_L^2+\mu_R^2)$ where the second term represents the chemical potential correction to the fermion conduction (here, the left-handed ones) and the last term arises from correction to the screenings (as will be seen in our explicit calculation later). Note that due to charge conjugation symmetry there will be no linear terms of $\mu_{L,R}$ in the expansion. Now the total vector current would then be $\boldsymbol{j}_V = \boldsymbol{j}_L + \boldsymbol{j}_R = \sigma(T;\mu_L,\mu_R)\boldsymbol{E} + \sigma(T;\mu_R,\mu_L)\boldsymbol{E} \approx [2\sigma_0 + (\sigma_0' + 2\sigma_0'')(\mu_V^2+\mu_A^2)]\,\boldsymbol{E}$ while the axial current would then be $\boldsymbol{j}_A = \boldsymbol{j}_R - \boldsymbol{j}_L \approx 4\sigma_0'\,\mu_V\mu_A\,\boldsymbol{E}$. We therefore see that its origin is not from the axial anomaly but from the conduction in a chiral many-body environment, and the CESE is completely different in nature from recently discussed axial current generation via anomaly in certain superfluid systems [32, 33].

Computation of the CESE Conductivity.—We will now compute explicitly the leading-log order CESE conductivity for thermal QED plasma using the Kubo formula under the condition $\mu_V, \mu_A \ll T$. The extension of this computation to QCD is straightforward, and will be presented elsewhere.

Let us denote $\sigma_e = \chi_e\mu_V\mu_A$. Starting with the retarded vector-vector and vector-axial correlators G^{Rij}_{VV} and G^{Rij}_{VA} (as diagrammatically shown in Fig. 1), the σ and σ_e are given via the Kubo formulae as:

$$\sigma = \sum_{i=1}^{3} \lim_{\omega\to 0}\lim_{\boldsymbol{k}\to 0} \frac{i}{3\omega} G^{Rii}_{VV}(\omega,\boldsymbol{k}), \tag{6}$$

$$\sigma_e = \sum_{i=1}^{3} \lim_{\omega\to 0}\lim_{\boldsymbol{k}\to 0} \frac{i}{3\omega} G^{Rii}_{AV}(\omega,\boldsymbol{k}), \tag{7}$$

In Fig. 1, the shaded circle represents an effective vertex, see Fig. 2. This effective vertex represents a resummation of a set of ladder diagrams which contribute to the same order owing to the pinching singularity when $\omega, \boldsymbol{k} \to 0$ [34]. The dotted line in Fig. 2 represents the hard thermal loop (HTL) resummed propagator. All other kinds of diagrams (e.g., the box diagrams which are vanishing identically due to Furry theorem at zero chemical potentials but finite at nonzero chemical potentials) are sub-leading-log order.

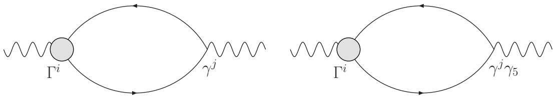

FIG. 1: The Feynmann diagrams for retarded correlators G^R_{VV} (Left) and G^R_{AV} (Right).

One can write down the retarded correlators explicitly:

$$G^{ij}_{VV} = -e\int_P \mathrm{Tr}\left[\Gamma^i(P+K,P)S(P)\gamma^j S(P+K)\right], \tag{8}$$

$$G^{ij}_{VA} = -e\int_P \mathrm{Tr}\left[\Gamma^i(P+K,P)S(P)\gamma^j\gamma_5 S(P+K)\right] \tag{9}$$

The effective vortex in the above is given by Fig. 2,

$$\Gamma^\mu(P+K,P) = \gamma^\mu + e^2\int_Q \gamma^\rho S(P+K+Q) \times\Gamma^\mu(P+K+Q,P+Q)S(P+Q)\gamma^\sigma {}^*D_{\rho\sigma}(Q). \tag{10}$$

The ${}^*D_{\rho\sigma}(Q)$ is the HTL propagator for photon while $S(P)$ is the electron propagator at nonzero μ_V and μ_A,

$$\begin{aligned} S(P) &= \frac{-1}{\gamma_0(p_0+\mu_V+\mu_A\gamma_5) - \boldsymbol{\gamma}\cdot\boldsymbol{p} - \gamma^\mu\Sigma_\mu(P)} \\ &= \sum_{s=\pm} \Xi_s \frac{-\gamma\cdot(P_s-\Sigma_s)}{(P_s-\Sigma_s)^2}, \end{aligned} \tag{11}$$

where $\Xi_\pm = (1\pm\gamma_5)/2$ is the chirality projection, $P^\mu_\pm = (P^0_\pm, \boldsymbol{p})$ with $P^0_\pm = p_0 + \mu_\pm$ and $\mu_\pm = \mu_V \pm \mu_A$. Substituting all these into the Kubo formulae and following essentially the steps as in Refs. [35, 36], we finally obtain,

$$\sigma = \sum_{s,a=\pm} \sigma_{sa}, \tag{12}$$

$$\sigma_e = \sum_{s,a=\pm} s\sigma_{sa}, \tag{13}$$

$$\sigma_{sa} = -a\frac{e}{3}\int \frac{d^3\boldsymbol{p}}{(2\pi)^3} n_F'(p-a\mu_s)\chi^s_a(p), \tag{14}$$

with $n_F(x) = 1/[\exp(x/T)+1]$ and $\chi^s_a(p) = \mathcal{D}^s_a(\boldsymbol{p})/\Gamma^s_a$. The $\mathcal{D}^s_a$ is defined through $2p^i\mathcal{D}^s_+(\boldsymbol{p}) = \bar{u}_s(\boldsymbol{p})\Gamma^i_+(\boldsymbol{p})u_s(\boldsymbol{p})$, $2p^i\mathcal{D}^s_-(\boldsymbol{p}) = \bar{v}_{-s}(-\boldsymbol{p})\Gamma^i_-(\boldsymbol{p})v_{-s}(-\boldsymbol{p})$, with $\Gamma^s_\pm = -2\mathrm{Im}\Sigma^R_{\pm s}(p^s_0 = \pm E_p, \boldsymbol{p})$ the decay width for fermions (+) and anti-fermions (−) of chirality s.

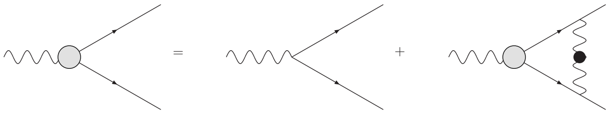

FIG. 2: Integral equation for the effective vertex Γ^μ.

The vertex integral equation (10) can be finally recast into a differential equation for $\chi^s_a(p)$:

$$\begin{aligned} 1 \ &= \ \frac{2\alpha m_s^2\ln(1/e)}{p}[n_B(p)+n_F(\mu_s)]\chi^s_a(p) \\ &+\frac{\alpha T m_D^2\ln(1/e)}{p^2}\Bigg[\chi^s_a(p) - \frac{p^2}{2}\frac{d^2\chi^s_a(p)}{dp^2} \\ &-\left(1-\frac{p}{2T}(1-2n_F[p-a\mu_s])\right)p\frac{d\chi^s_a(p)}{dp}\Bigg], \quad (15)\end{aligned}$$

where $n_B(x) = 1/[\exp(x/T)-1]$ is the Bose-Einstein function, $\alpha = e^2/4\pi$, $m_s^2 = \frac{e^2}{8}\left(T^2+\frac{\mu_s^2}{\pi^2}\right)$ is the effective mass of electrons, $m_D^2 = \frac{e^2}{6}\sum_{s=\pm}\left(T^2+\frac{3\mu_s^2}{\pi^2}\right)$ is the Debye screening mass of photons. We note that the leading-order terms in the effective vertex and those in the fermion decay width cancel each other and as a result the leading-log results for conductivities are actually at the order $\hat{O}(1/[e^3\ln(1/e)])$ rather than $\hat{O}(1/[e\ln(1/e)])$ as expected from $\sigma_{sa}\sim e/\Gamma^s_a$.

Following Ref. [37], we solve this differential equation numerically by using variational method. This variational scheme converges very fast, and at very high precision we obtain (up to $\hat{O}(\mu_s/T)^2$ order)

$$\begin{aligned}\sigma_{sa} \approx \frac{T}{e^3\ln(1/e)}\Bigg(&3.9238+4.59867a\frac{\mu_s}{T}+2.56237\frac{\mu_s^2}{T^2} \\ &-0.62224\frac{\mu_V^2+\mu_A^2}{T^2}\Bigg), \quad (16)\end{aligned}$$

and thus

$$\begin{aligned}\sigma \ &\approx \ \frac{T}{e^3\ln(1/e)}\left(15.6952+7.76052\frac{\mu_V^2+\mu_A^2}{T^2}\right), \quad (17) \\ \sigma_e \ &\approx \ 20.499\frac{\mu_V\mu_A}{T^2}\frac{T}{e^3\ln(1/e)}. \quad (18)\end{aligned}$$

In the limit $\mu_s\to 0$, our result for σ is in agreement with $\sigma\approx 15.6964\frac{T}{e^3\ln(1/e)}$ obtained in Ref. [37].

Coupled Evolution of the Two Currents.— As seen in Eq.(5), with the presence of external electromagnetic fields, the vector and axial currents mutually induce each other and get entangled in a nontrivial way. It is of great interest to understand the coupled evolution of small fluctuations of the two currents. A very good example is the aforementioned CMW [29, 30] in which the fluctuations of vector and axial currents are coupled together by external $\boldsymbol{B}$ field to form a propagating wave. Now the new CESE effect introduces nonlinearity (aka the $\mu_V\mu_A$ term) and makes the problem more nontrivial.

Let us consider a thermal QED or QCD plasma in the static and homogeneous external $\boldsymbol{E},\boldsymbol{B}$ fields, and study the coupled evolution of the small fluctuations in vector and axial charge densities. The presence of vector density and current will induce additional electromagnetic fields so that $\boldsymbol{E}_{\rm tot} = \boldsymbol{E}+\delta\boldsymbol{E}$ and $\boldsymbol{B}_{\rm tot} = \boldsymbol{B}+\delta\boldsymbol{B}$ with $\delta\boldsymbol{E}\propto ej^0_V$ and $\delta\boldsymbol{B}\propto e\boldsymbol{j}_V$. As in the case of CMW, one can first replace the chemical potentials in Eq.(5) with the corresponding charge densities: $\mu_{V,A} = \alpha_{V,A}j^0_{V,A}$, where the $\alpha_{V,A}$ are the susceptibilities defined as $\alpha_{V,A}\equiv\partial\mu_{V,A}/\partial j^0_{V,A}$. These relations are valid as long as the chemical potentials are small compared with temperature T. Then, combining Eq.(5) with the currents' continuity equations $\partial_t j^0_{V,A}+\bigtriangledown\cdot\boldsymbol{j}_{V,A}=0$ and Maxwell's equation $\bigtriangledown\cdot\boldsymbol{E}_{\rm tot} = ej^0_V$ and $\bigtriangledown\cdot\boldsymbol{B}_{\rm tot}=0$, one can obtain:

$$\begin{aligned}&\partial_t j^0_V + e\sigma_0 j^0_V + \sigma_5\alpha_A(\boldsymbol{B}\cdot\bigtriangledown)j^0_A \\ &+2\sigma_2\alpha_V^2 j^0_V(\boldsymbol{E}\cdot\bigtriangledown)j^0_V + 2\sigma_2\alpha_A^2 j^0_A(\boldsymbol{E}\cdot\bigtriangledown)j^0_A = 0\,, \\ &\partial_t j^0_A + \sigma_5\alpha_V(\boldsymbol{B}\cdot\bigtriangledown)j^0_V + \chi_e\alpha_V\alpha_A j^0_V(\boldsymbol{E}\cdot\bigtriangledown)j^0_A \\ &+\chi_e\alpha_V\alpha_A j^0_A(\boldsymbol{E}\cdot\bigtriangledown)j^0_V = 0\,. \quad (19)\end{aligned}$$

where we have introduced σ_0 and σ_2 defined through the small chemical potential expansion of σ, $\sigma = \sigma_0+\sigma_2(\mu_V^2+\mu_A^2)$. In arriving at the above, we have made a few approximations: first we keep only terms up to $\hat{O}(j^2_{V,A})$ order (such that terms like $j^0\delta\boldsymbol{E}\cdot\bigtriangledown j^0\sim\hat{O}(j^3)$ and $\sigma_2\mu^2 j^0_V$ are dropped); second we assume external fields are extremely strong such that the magnetic field feedback terms $\sim\sigma_5\alpha\delta\boldsymbol{B}\cdot\bigtriangledown j^0\sim\sigma_5\alpha e(j\partial j)$ are negligible to other $\hat{O}(j^2)$ terms $\sim\chi_e\alpha^2 E(j\partial j)$ and $\sim\sigma_2\alpha^2 E(j\partial j)$. We will next linearize the above equations by considering fluctuations on top of small uniform background vector and axial densities n_V and n_A, so that $j^0_{V,A} = n_{V,A}+\delta j^0_{V,A}$ with $\delta j^0_{V,A}\ll n_{V,A}$ being fluctuations. Note that $n_{V,A}$ themselves must still be small (compared to T^3) to ensure the linear relations between $j^0_{V,A}$ and $\mu_{V,A}$. Strictly speaking only a uniform axial density n_A is a static solution of the above equations while a uniform vector density n_V suffers from the damping term $e\sigma_0 j^0_V$ and is only approximately static on time scale shorter compared with $1/e\sigma_0$. Keeping only linear terms in $\delta j^0_{V,A}$ we obtain:

$$\begin{aligned}&\partial_t\delta j^0_V + e\sigma_0\delta j^0_V + \sigma_5\alpha_A(\boldsymbol{B}\cdot\bigtriangledown)\delta j^0_A \\ &\quad+2\sigma_2\alpha_V^2 n_V(\boldsymbol{E}\cdot\bigtriangledown)\delta j^0_V + 2\sigma_2\alpha_A^2 n_A(\boldsymbol{E}\cdot\bigtriangledown)\delta j^0_A = 0\,, \\ &\partial_t\delta j^0_A + \sigma_5\alpha_V(\boldsymbol{B}\cdot\bigtriangledown)\delta j^0_V + \chi_e\alpha_V\alpha_A n_V(\boldsymbol{E}\cdot\bigtriangledown)\delta j^0_A \\ &\quad+\chi_e\alpha_V\alpha_A n_A(\boldsymbol{E}\cdot\bigtriangledown)\delta j^0_V = 0\,. \quad (20)\end{aligned}$$

In order to find possible normal modes, we make the Fourier transformation of these equations. Using $\delta j^0_{V,A} =$

$\int_{\omega,\boldsymbol{k}} C_{V,A}(\omega,\boldsymbol{k})\, e^{-i(\omega t-\boldsymbol{k}\cdot\boldsymbol{x})}$, we obtain from Eqs. (20) the following relations:

$$\begin{aligned}
&\omega C_V + ie\sigma_0 C_V - \sigma_5\alpha_A(\boldsymbol{B}\cdot\boldsymbol{k})C_A \\
&\quad -2\sigma_2\alpha_V^2 n_V(\boldsymbol{E}\cdot\boldsymbol{k})C_V - 2\sigma_2\alpha_A^2 n_A(\boldsymbol{E}\cdot\boldsymbol{k})C_A = 0\,, \\
&\omega C_A - \sigma_5\alpha_V(\boldsymbol{B}\cdot\boldsymbol{k})C_V - \chi_e\alpha_V\alpha_A n_A(\boldsymbol{E}\cdot\boldsymbol{k})C_V \\
&\quad -\chi_e\alpha_V\alpha_A n_V(\boldsymbol{E}\cdot\boldsymbol{k})C_A = 0\,. \qquad (21)
\end{aligned}$$

Without loss of generality, we can always assume $\boldsymbol{B}$ is along z-axis, i.e., $\boldsymbol{B} = B\hat{z}$ while $\boldsymbol{E} = E\hat{e}$. The dispersion relation obtained from Eq. (21) can be expressed as

$$\begin{aligned}
\omega = &-\frac{1}{2}\left[ie\sigma_0 - v_+(\hat{e}\cdot\boldsymbol{k})\right] \\
&\pm\frac{1}{2}\sqrt{\left[ie\sigma_0 - v_-(\hat{e}\cdot\boldsymbol{k})\right]^2 + 4\mathcal{A}_\chi(\boldsymbol{k})}, \qquad (22)
\end{aligned}$$

where $v_\pm = v_v \pm v_a$ with $v_v = 2\sigma_2\alpha_V^2 n_V E$ and $v_a = \chi_e\alpha_V\alpha_A n_V E$, and

$$\begin{aligned}
\mathcal{A}_\chi(\boldsymbol{k}) \;=\; &\left[\sigma_5\alpha_A B(\hat{z}\cdot\boldsymbol{k}) + 2\sigma_2\alpha_A^2 n_A E(\hat{e}\cdot\boldsymbol{k})\right] \\
&\times\left[\sigma_5\alpha_V B(\hat{z}\cdot\boldsymbol{k}) + \chi_e\alpha_V\alpha_A n_A E(\hat{e}\cdot\boldsymbol{k})\right] . (23)
\end{aligned}$$

To manifest the physical meaning of the solutions in (22), let us consider two special cases.

(1) The case with only $\boldsymbol{B} = B\hat{z}$ and $\boldsymbol{E} = 0$. Then Eq.(22) reduces to $\omega = \pm\sqrt{(v_\chi k_z)^2 - (e\sigma_0/2)^2} - i(e\sigma_0/2)$ with speed $v_\chi = \sigma_5\sqrt{\alpha_V\alpha_A}B$. When $v_\chi k_z \gg e\sigma_0/2$ we get two well-defined propagating modes $\omega \approx \pm v_\chi k_z - i(e\sigma_0/2)$: these are generalized CMWs which reduce to the CMW in [29] when $\sigma_0 = 0$ and $\alpha_V = \alpha_A$. When $v_\chi k_z \le e\sigma_0/2$ the two modes become purely damped.

(2) The case with only $\boldsymbol{E} = E\hat{z}$ and $\boldsymbol{B} = 0$. First, we consider a background without vector density, i.e., $n_V = 0$. In this case, we find two modes from (22)

$$\omega = \pm\sqrt{(v_e k_z)^2 - (e\sigma_0/2)^2} - i(e\sigma_0/2) \qquad (24)$$

with $v_e = \alpha_A n_A\sqrt{2\sigma_2\chi_e\alpha_V\alpha_A}E$. Similar to the CMWs, when $v_e k_z \gg e\sigma_0/2$ there are two well-defined modes $\omega \approx \pm v_e k_z - i(e\sigma_0/2)$ from CESE that propagate along $\boldsymbol{E}$ field and can be called the Chiral Electric Waves (CEWs). They become damped when $v_e k_z \le e\sigma_0/2$.
Second, if the background contains no axial density, i.e., $n_A = 0$, then we see that the vector and axial modes become decoupled, and Eq. (22) leads to

$$\begin{aligned}
\omega_V(\boldsymbol{k}) &= v_v k_z - i(e\sigma_0)\,, \\
\omega_A(\boldsymbol{k}) &= v_a k_z. \qquad (25)
\end{aligned}$$

The first solution $\omega_V(\boldsymbol{k})$ represents a "vector density wave" (VDW) with speed $v_v = 2\sigma_2\alpha_V^2 n_V E$ that transports vector charges along $\boldsymbol{E}$ field but will be damped on a time scale $\sim 1/(e\sigma_0)$. The second solution $\omega_A(\boldsymbol{k})$ is a new mode arising from CESE and represents a propagating "axial density wave" (ADW) along $\boldsymbol{E}$ with speed $v_a = \chi_e\alpha_V\alpha_A n_V E$ and without damping.

Summary and Discussions.—In summary, we have found a new mechanism for the generation of axial current by external electric field in a conducting matter with nonzero vector and axial charge densities, which we call the Chiral Electric Separation Effect. We have computed the CESE conductivity coefficient in a QED plasma and also studied possible collective mode arising from it.

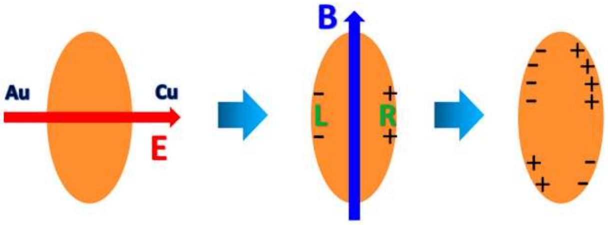

FIG. 3: A schematic illustration for CESE induced net charge distribution and correlation patterns in Cu + Au collision.

We end by discussing possible observable effect that may be induced by CESE in heavy ion collisions. In the created hot QGP there can be both vector and axial charge densities from fluctuations and topological transitions. There are also very strong electric fields during the early moments of heavy ion collisions [20–22, 24]. One particularly interesting situation is in the Cu + Au collisions, where due to the asymmetric nuclei (rather than from fluctuations) there will be a strong $\boldsymbol{E}$ field directing from Au nucleus to Cu nucleus [40]. In this case the $\boldsymbol{E}$ field will lead to both an in-plane charge separation via (1) and an in-plane chirality separation via (4). The resulting in-plane axial dipole will then further separate charges via CME along the magnetic field in the out-of-plane direction, and cause an approximate quadrupole at certain angle Ψ_q in between in- and out-of-plane . We therefore expect a highly nontrivial charge azimuthal distribution pattern $\delta N_\pm(\phi) \sim d\cos(\phi) + q\cos(2\phi - 2\Psi_q)$ with the dipole term due to usual conductivity and the quadrupole term due to CESE and CME effects. This pattern may possibly be measured either via charged pair correlations or the charged multiple analysis [22]. More quantitative predictions will require proper modeling of the QGP and solving the Eq. (20) which will be reported in a future work.

Acknowledgments— We thank Dmitri Kharzeev, Shu Lin, Misha Stephanov, and Ho-Ung Yee for helpful discussions. J.L. is grateful to the RIKEN BNL Research Center for partial support.

---

[*] Electronic address: `xuhuang@indiana.edu`
[†] Electronic address: `liaoji@indiana.edu`

[1] D. Kharzeev, Phys. Lett. B **633**, 260 (2006).
[2] D. Kharzeev and A. Zhitnitsky, Nucl. Phys. A **797**, 67 (2007).

[3] D. E. Kharzeev, L. D. McLerran and H. J. Warringa, Nucl. Phys. A **803**, 227 (2008).

[4] K. Fukushima, D. E. Kharzeev and H. J. Warringa, Phys. Rev. D **78**, 074033 (2008).

[5] D. E. Kharzeev, Annals Phys. **325**, 205 (2010).

[6] D. T. Son and A. R. Zhitnitsky, Phys. Rev. D **70**, 074018 (2004).

[7] M. A. Metlitski and A. R. Zhitnitsky, Phys. Rev. D **72**, 045011 (2005).

[8] H. U. Yee, JHEP **0911**, 085 (2009).

[9] A. Rebhan, A. Schmitt and S. A. Stricker, JHEP **1001**, 026 (2010).

[10] V. A. Rubakov, arXiv:1005.1888 [hep-ph].

[11] A. Gynther, K. Landsteiner, F. Pena-Benitez and A. Rebhan, JHEP **1102**, 110 (2011).

[12] A. Gorsky, P. N. Kopnin and A. V. Zayakin, Phys. Rev. D **83**, 014023 (2011).

[13] A. V. Sadofyev and M. V. Isachenkov, Phys. Lett. B **697**, 404 (2011); A. V. Sadofyev, V. I. Shevchenko, and V. I. Zakharov, Phys. Rev. D **83**, 105025 (2011); V. P. Kirilin, A. V. Sadofyev and V. I. Zakharov, Phys. Rev. D **86**, 025021 (2012).

[14] T. Kalaydzhyan and I. Kirsch, Phys. Rev. Lett. **106**, 211601 (2011); I. Gahramanov, T. Kalaydzhyan, and I. Kirsch, Phys. Rev. D **85**, 126013 (2012).

[15] J. H. Gao, Z. T. Liang, S. Pu, Q. Wang and X. N. Wang, Phys. Rev. Lett. **109**, 232301 (2012); J. -W. Chen, S. Pu, Q. Wang and X. -N. Wang, arXiv:1210.8312 [hep-th].

[16] D. T. Son and N. Yamamoto, Phys. Rev. Lett. **109**, 181602 (2012); arXiv:1210.8158 [hep-th].

[17] M. A. Stephanov and Y. Yin, Phys. Rev. Lett. **109**, 162001 (2012).

[18] P. V. Buividovich, M. N. Chernodub, E. V. Luschevskaya and M. I. Polikarpov, Phys. Rev. D **80**, 054503 (2009).

[19] M. Abramczyk, T. Blum, G. Petropoulos and R. Zhou, PoS **LAT2009**, 181 (2009).

[20] A. Bzdak and V. Skokov, Phys. Lett. B **710**, 171 (2012).

[21] W. T. Deng and X. G. Huang, Phys. Rev. C **85**, 044907 (2012).

[22] J. Bloczynski, X. G. Huang, X. Zhang and J. Liao, Phys. Lett. B **718**, 1529 (2013).

[23] K. Tuchin, Phys. Rev. C **82**, 034904 (2010) [Erratum-ibid. C **83**, 039903 (2011)].

[24] V. Voronyuk, V. D. Toneev, W. Cassing, E. L. Bratkovskaya, V. P. Konchakovski and S. A. Voloshin, Phys. Rev. C **83**, 054911 (2011).

[25] B. I. Abelev *et al.* [STAR Collaboration], Phys. Rev. Lett. **103**, 251601 (2009). B. I. Abelev *et al.* [STAR Collaboration], Phys. Rev. C **81**, 054908 (2010).

[26] N. N. Ajitanand, R. A. Lacey, A. Taranenko and J. M. Alexander, Phys. Rev. C **83**, 011901 (2011).

[27] B. Abelev *et al.* [ALICE Collaboration], Phys. Rev. Lett. **110**, 012301 (2013) [arXiv:1207.0900 [nucl-ex]].

[28] A. Bzdak, V. Koch and J. Liao, Phys. Rev. C **81**, 031901 (2010); Phys. Rev. C **82**, 054902; arXiv:1207.7327 [nucl-th]. B. Muller, A. Schafer and , Phys. Rev. C **82**, 057902 (2010). S. Schlichting, S. Pratt and , Phys. Rev. C **83**, 014913 (2011). F. Wang, Phys. Rev. C **81**, 064902 (2010).

[29] D. E. Kharzeev and H. U. Yee, Phys. Rev. D **83**, 085007 (2011).

[30] Y. Burnier, D. E. Kharzeev, J. Liao and H. U. Yee, Phys. Rev. Lett. **107**, 052303 (2011); arXiv:1208.2537 [hep-ph].

[31] G. Wang [STAR Collaboration], arXiv:1210.5498 [nucl-ex].

[32] Y. Neiman and Y. Oz, JHEP **1109**, 011 (2011).

[33] S. Lin, Nucl. Phys. A **873**, 28 (2012).

[34] S. Jeon, Phys. Rev. D **52**, 3591 (1995).

[35] M. A. Valle Basagoiti, Phys. Rev. D **66**, 045005 (2002).

[36] G. Aarts and J. M. Martinez Resco, JHEP **0211**, 022 (2002).

[37] P. B. Arnold, G. D. Moore and L. G. Yaffe, JHEP **0011**, 001 (2000).

[38] S. Lin, Phys. Rev. D **85**, 045015 (2012).

[39] G. M. Newman, JHEP **0601**, 158 (2006).

[40] Y. Hirono, M. Hongo and T. Hirano, arXiv:1211.1114 [nucl-th].